A Power Allocation-Based Overlapping Transmission Scheme in Internet of Vehicles

Dalong Zhang, Liming Zheng, Qixiao Chen, Baodian Wei, and Xiao Ma, *Member, IEEE*

***Abstract*—Internet of Vehicles (IoV) is the basis of future intelligent transportation systems. Both the control signaling and data dissemination services in IoV must be transmitted with high reliability and low latency so that safety can be guaranteed. Based on the discussion and analyses of issues in achieving high reliability low latency transmissions, we present in this paper a Polar code-based overlapping transmission scheme in which simultaneous transmissions from different nodes to the same receiving node are allowed to use the same time-frequency resource block. To effectively eliminate multiple access interference introduced by the overlapped nonorthogonal transmissions, a successive cancellation list-based improved interference elimination decoding algorithm (SCL-based IIEDA) is proposed to retrieve the Polar coded information. Numerical results show that the SCL-based IIEDA performs well on information recovery in the presented transmission scheme. In addition, it is shown that the proposed scheme not only significantly reduces the acknowledgment overhead but also greatly improves the spectral efficiency.**

***Index Terms*—Control and data dissemination services, Internet of Vehicles (IoV), nonorthogonal multiple access, overlapping transmission, Polar code.**

I. Introduction

THE CONCEPT of Internet of Vehicles (IoV), as a core component of the future intelligent transportation systems, has been attracting increasing interests from both academia and industry in the past few years [1]–[3]. According to the 3rd Generation Partnership Project (3GPP) [4], [5], the fifth generation (5G) cellular mobile communication networks are envisaged to expand and support diverse application scenarios and services, including enhanced mobile broadband, massive machine type communications, and ultrareliable and low-latency communications (uRLLC) [4], [5]. The IoV is regarded as one of the typical 5G application scenarios of uRLLC [6]. Meanwhile, the bandwidth-extensive applications (e.g., exchange of video captured onboard, digital map downloading, and onboard navigation) are also the future requirements of the IoV. Due to the limitation of wireless channel resources, it is particularly important to improve the channel utilization [7]. A typical IoV system is composed of multiple users and multiple vehicles. In IoV system, interaction between the transportation infrastructure and multiple networks may also be involved. With an open and self-organizing network structure, it is important to achieve high reliability low latency transmissions in IoV such that manageability, controllability, and credibility of the system can be achieved.

Recent studies show that control signaling and data dissemination are the two key services of IoV [8]–[10]. Both services generally involve delivery of information to multiple receiving nodes (RNs). If the quality-of-service (QoS) requirement in terms of transmission reliability is low, broadcast schemes can be used to minimize latency and overhead. However, such best-effort broadcast services cannot provide guaranteed QoS to successfully deliver all packets to all the RNs. To solve this problem, unicast is usually employed to improve transmission reliability in existing wireless communication systems. In this case, the source node successively transmits the service packets to each RN and waits for an acknowledgment (ACK) packet as a response. The transmission of a large number of ACK packets will occupy a large amount of wireless channel resources, resulting in high ACK overhead, low channel utilization, and long transmission delay. In future IoV application scenarios, the nodes are densely deployed, the moving speed of the nodes is fast, and topology of the network changes rapidly. Meanwhile, because of the self-organizing nature of IoV, the control and data dissemination service packets will also experience contention, collision, and congestion. As a result, it will be more difficult to be guaranteed the transmission reliability and latency.

To solve the above problems for future IoV, many existing works have been focused on improving transmission reliability in broadcasting. Solutions including optimal backbone-based broadcasting [11], network coding-based retransmission [12], and reliable broadcast channel scheduling [13] have been investigated. However, to improve the reliability of information

Manuscript received April 16, 2018; revised August 13, 2018; accepted September 20, 2018. Date of publication October 1, 2018; date of current version February 25, 2019. This work was supported in part by the National Science Foundation of China under Grant 91438101, in part by the National Science and Technology Major Projects of China under Grant 2017ZX03001001-004, in part by the EU's Horizon 2020 Research and Innovation Staff Exchange programme (TESTBED Project) under Grant 734325, in part by the China-EU Intergovernmental Cooperation Project under Grant 2017YFE0112600, in part by the Fundamental Research Funds for the Central Universities under Grant 17lgjc22, in part by Guangdong NSF under Grant 2016A030313298, and in part by the Opening Fund of Qiongqing Key Laboratory of Computer Network and Communication Technology under Grant CY-CNCL-2017-04. *(Corresponding author: Liming Zheng.)*

D. Zhang is with the School of Information Engineering, Zhengzhou University, Zhengzhou 450001, China (e-mail: iedlzhang@zzu.edu.cn).

L. Zheng, Q. Chen, and X. Ma are with the School of Data and Computer Science, Sun Yat-sen University, Guangzhou 510006, China (e-mail: zhenglm7@mail2.sysu.edu.cn; chenqx27@mail2.sysu.edu.cn; maxiao@mail.sysu.edu.cn).

B. Wei is with the Chongqing Key Laboratory of Computer Network and Communication Technology, School of Computer Science and Technology, Chongqing University of Posts and Telecommunications, Chongqing 400065, China (e-mail: weibd@mail.sysu.edu.cn).

Digital Object Identifier 10.1109/JIOT.2018.2873480

delivery, the ACK mechanism is still the most effective choice. Generally, there are multiple RNs in broadcast services. Due to the contention and collision problems, it is a challenge that all neighboring nodes successfully received the broadcast packet and replied an ACK packet in a dense and dynamic IoV network. An alternative solution is to ask the RNs to send ACKs one by one in a certain way. This approach requires sophisticated designs for queuing, scheduling and ordering, which is also a challenge in self-organizing networks. Especially when the number of RNs is large, it will lead to significant system overhead and long delay. Specifically, the transmission latency of conventional ACK-based scheme consists of two parts: 1) the transmission time of a broadcast packet and 2) response time of ACK packets. The response time of ACK packets is denoted by $n*(\mathrm{IFS}+\mathrm{ACK})$, where n is the number of RNs, IFS denotes the time duration for interframe space, and ACK denotes the time elapsed during an ACK packet transmission. In view of the mentioned problems in broadcast services, if it is possible to implement overlapping transmission of the ACK packets, it will surely reduce the packet transmission latency and the corresponding system overhead. Reducing the overhead is equivalent to improving the channel utilization. Therefore, in this paper, we introduce the nonorthogonal overlapping transmission for ACK packets to facilitate high reliability low latency transmissions of the control and data dissemination services in IoV. To comply with standardization initiatives for signaling over 5G air interface, Polar code is employed in the proposed scheme. Meanwhile, the control and data dissemination service packets may also be forwarded by multiple relay nodes. If overlapping transmission can be used, the spectral efficiency will be greatly improved and the transmission latency will be further reduced.

To recover information from overlapped signals, many related works based on different encoding and decoding techniques have been reported [14]–[18]. Hoeher and Wo [14] discussed nonobjective modulation and showed a universal model for superposition modulation and *a posteriori* probability detection technique. Zhu *et al.* [15] proposed an overlapping transmission scheme for throughput enhancement in sensor networks where each layer of the overlapped signal is from different sensor nodes. Zhao *et al.* [16] designed decoding algorithms for superposition modulation system. A computing-based iterative multistage decoding algorithm and a joint decoding scheme for overlapped signals recovery were proposed on the basis of LDPC decoding. Based on the idea of superposition modulation, Ishii [17] proposed a modulation and detection scheme to achieve cooperative transmit diversity. Through carefully designed power allocation, the RN can recover overlapped transmitted signals by calculating the log-likelihood ratio in the decoding process. Larsson and Vojcic [18] also studied cooperative transmit diversity with superposition modulation. By cooperative forwarding of superposition modulated packets, the decoder at the receiver can recover the information from the contiguous packets.

Polar code is a capacity-achieving error correcting code proposed by Arikan [19] and Korada [20]. Recently, Polar code has been adopted by 3GPP as the channel coding scheme for control signaling over the 5G new air interface [21]. The original idea of Polar code can be traced back to Arikan's earlier work on improving the sum cutoff rate of channels by the channel combining and splitting method [22]. In [22], a simple linear transformation was applied to the inputs before transmission, and a successive cancellation-type decoder was used at the channel output. The original bit channels can be combined by the simple linear transformation and then split into correlated subchannels seen by the bit. The idea of Polar codes is based on recursively repeating the above simple transformation. The recursive process applies the linear transformation to a larger number of bits at the encoder. At the decoder, the bits can be decoded successively in a particular order. The effective channels seen by some of the bits are better than original channel, and some are worse. As the block length increases, these effective channels tend to become either a completely noisy channel or a noiseless channel with the fraction of noiseless channels approaching the capacity of original channel. This phenomenon is referred to as channel polarization. This suggests a simple scheme where we fix the frozen bits to the channels that are bad and transmit information bits over the noiseless channels without any coding. The codes in the scheme are the Polar codes. Such a scheme has been proved to approach the capacity of the channel.

The objective of this paper is to use Polar code in overlapped transmissions to overcome the above mentioned problems in IoV. The main contributions of this paper include the following.

1) We present a Polar code-based overlapping transmission scheme to reduce overhead and delay for IoV services.
2) We present a successive cancellation list-based improved interference elimination decoding algorithm (SCL-based IIEDA) for information recovery in the overlapping transmission scheme.
3) Through numerical studies, it is revealed that the proposed scheme works well even when two signals from different nodes are entirely overlapped.

The rest of this paper is organized as follows. In Section II, we present the basic system model and the symbol definitions in this paper. The decoding process and the corresponding algorithms are presented in Section III. We demonstrate the performance of our proposed scheme in Section IV through numerical examples. Finally, this paper is concluded in Section V.

II. System Model

A. Overview of the Previous Reliable Broadcast Transmission

In IoV, the ACK mechanism is the most effective way to guarantee the reliability of packet broadcasting. However, the high signaling overhead and long transmission delay must be addressed to meet the low latency requirement of the uRLLC services. As shown in Fig. 1, there are densely deployed IoV nodes in typical IoV scenarios. The number of one-hop neighbor vehicles of a broadcasting node is typically large. As the number of one-hop neighboring vehicles increases, the time elapsed for one by one ACK packet transmission

increasing rapidly. Furthermore, due to the fast fading nature of IoV channels [23], [24], expanding the transmission latency window will lead to detrimental impact on the transmission reliability. Ultrahigh reliability and low latency are therefore conflicting the requirements in this scenario.

A MAC header additional field named ACK Order is usually used to avoid the ACK packet collisions. After receiving the broadcast packet, neighboring vehicles which are specified in the ACK Order will reply with an ACK one by one according to the order indicated by the broadcasting node in the ACK Order field.

For existing reliable broadcast services adopting the ACK mechanism, we have the following assumptions.

1) The service packets and ACK packets share the same channel.
2) The broadcasting node can obtain the information of one-hop neighboring vehicles, which include the number and ID of all neighboring vehicles. The neighboring vehicles' information is mainly used to determine the ACK Order.
3) The broadcast nodes use carrier sense multiple access mechanism to access the wireless channel. The impact of channel collisions is ignored for the broadcast data packets and the ACK packets.
4) According to the IEEE 802.11p protocol [25], the frame format of ACK packet is shown in Fig. 2. If we assume the length of ACK packet is 112 bits, by making encoding using the Polar code of rate 0.5, the packet length becomes 224 bits.
5) Based on the transmission latency normalization, as shown in Fig. 1, we assume the transmission latency of ACK packets is 1, and the transmission latency of service data packets is 8.

Based on the above assumptions, if there are ten neighboring vehicles surrounding the broadcast node, the transmission latency introduced by the ACK process is 10. The total transmission latency, including transmission of the service data packets sending and the ACK packets, sum to 18. About 55.6% of the total transmission latency is contributed by the ACK process. On the other hand, if an overlapping ACK transmission scheme is adopted, the total transmission latency can be reduced to 13, where 5 is due to ACK packets transmissions. The fraction attributed to ACK transmissions in the total latency decreases to 38.5%. Therefore, the total transmission latency and overhead of reliable broadcast services can be reduced by adopting the overlapping transmission scheme.

B. System Assumptions

For ease of illustration, in this paper, we focus on the communication system as shown in Fig. 3(a), which involves two transmitting nodes (for ACK) and one RN, all equipped with single-antenna. Two data blocks are initiated independently at the two sending nodes (SNs), namely the zeroth SN and the first SN. The two signals sent from the zeroth SN and the first SN overlap in the channel while transmitting. The overlapped signal are finally received by the RN. The RN recovers the information from both the zeroth SN and the first SN from the received overlapped signals.

We make the following assumptions for the system.

1) Each of the SNs is with an identical structure and the messages of the SNs are (channel) encoded with Polar codes.
2) The channel state information is perfectly known by all nodes in this system.
3) Symbol synchronization has been established in the system to facilitate the recovery of overlapped signals.
4) The relative delay of the received signals from different SNs can be accurately estimated by the RN.

C. Sending Node Side

In order to improve the system throughput of IoV, every two SNs are allocated with different power levels and then send their packets to the RN using the same time-frequency resource block. A schematic of the communication system for data blocks is given in Fig. 3(b).

First, the ℓth SN attempts to transmit a binary information sequence $\underline{u}^{(\ell)} = (u_0^{(\ell)}, u_1^{(\ell)}, \ldots, u_K^{(\ell)})$ through the additive white Gaussian noise (AWGN) channel, where $\ell \in \{0, 1\}$. The binary vector $\underline{u}^{(\ell)}$ is then encoded into $\underline{c}^{(\ell)} = (c_0^{(\ell)}, c_1^{(\ell)}, \ldots, c_{N-1}^{(\ell)})$ using rate $R = K/N$ Polar code. Binary phase shift keying (BPSK) is used to modulate the encoded sequence into a bipolar signal vector $\underline{v}^{(\ell)} = (v_0^{(\ell)}, v_1^{(\ell)}, \ldots, v_{N-1}^{(\ell)})$, where $v_i^{(\ell)} = \phi(c_i^{(\ell)}) = 1 - 2c_i^{(\ell)}$ for $i = 0, 1, \ldots, N-1$. Given the amplitude $\alpha^{(\ell)}$, the signal $x_i^{(\ell)}$ is sent out at time $\tau^{(\ell)}$ with $x_i^{(\ell)} = \alpha^{(\ell)} v_i^{(\ell)}$. Note that the amplitude $\alpha^{(\ell)}$ is a parameter that can be adjusted by the ℓth SN. Although each of the SNs is with identical structure, the transmitting power $P^{(\ell)}$ of these nodes can be different.

D. Overlapping Model

In an ideal communication system, we hope that two SNs can send packets to the RN at exactly the same time. However, in practice, time synchronization between two SNs is usually difficult to be strictly guaranteed, especially in self-organizing networks. It results in different degrees of overlap between the two transmitted signals, which is illustrated in Fig. 4. Without loss of generality, we assume that $\tau^{(0)} = 0$. The relative delay of the two signals is denoted by $\Delta\tau = \tau^{(1)} - \tau^{(0)}$. According to the relative delay $\Delta\tau$, there are three cases detailed in the following.

1) Nonoverlapping Case: When the relative delay $\Delta\tau \geq N$, the transmissions are orthogonal. Consequently, there is no multiple access interference or overlap between the two signals. In this case, signal detection is relatively simple. The transmission process from the SNs to the RN can be viewed as independent point-to-point transmissions.

2) Partially Overlapping Case: When the two SNs transmit with a relative delay $\Delta\tau$, where $1 \leq \Delta\tau < N$, a portion of the two signals is overlapped. That is to say, there is a mutual interference between the two signals. We call this case partially overlapping transmission.

3) Entirely Overlapping Case: Considering the ideal situation that the two SNs transmit to the RN at exactly the same

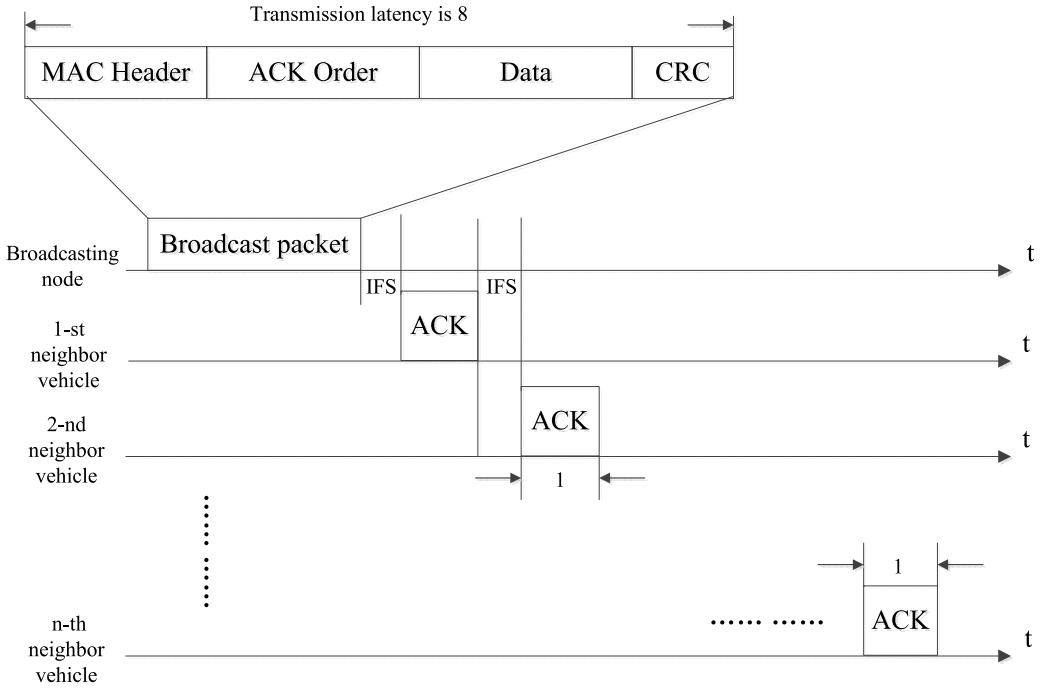

Fig. 1. Current ACK sending process and the frame structure of broadcast packet. IFS is the interframe space whose length is determined by state switching and processing delay, etc.

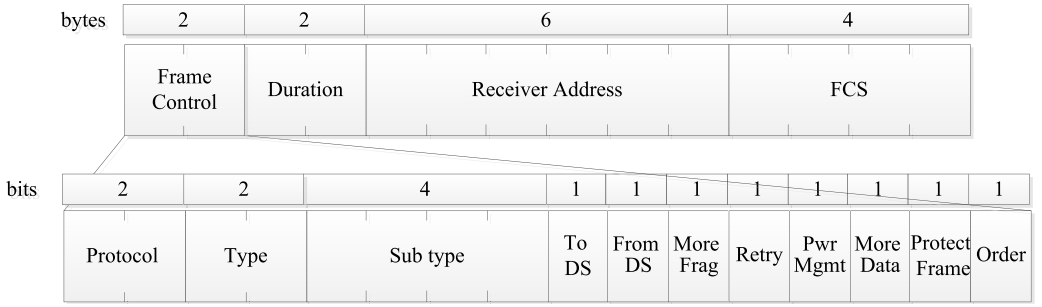

Fig. 2. Frame structure in IEEE 802.11p protocol.

time instantly, the signals from the two SNs are completely overlapped and the relative delay $\Delta\tau$ is zero. We call this scenario entirely overlapping transmission.

Let $\mathcal{L}_t$ denote the set of the indices of SNs which are *active* (transmitting packets) at time instant t. We observe in Fig. 4 that $\mathcal{L}_t = \{0\}$ for $0 \le t < \Delta\tau$, $\mathcal{L}_t = \{0, 1\}$ for $\Delta\tau \le t < N$, and $\mathcal{L}_t = \{1\}$ for $N \le t < N + \Delta\tau$. The received signals at the RN is denoted by $\underline{y} = (y_0, y_1, \ldots, y_{N+\Delta\tau-1})$ with

$$y_t = \sum_{\ell\in\mathcal{L}_t} x^{(\ell)}_{t-\tau^{(\ell)}} + z_t = \sum_{\ell\in\mathcal{L}_t} \alpha^{(\ell)}_{t-\tau^{(\ell)}} \left(1 - 2c^{(\ell)}_{t-\tau^{(\ell)}}\right) + z_t \qquad (1)$$

where z_t, for $0 \le t < N + \Delta\tau$, is a sample from an AWGN ensemble with variance $\sigma^2 = (N_0/2)$.

When the relative delay $\Delta\tau \ge N$, there is no transmission overlap between the two SNs. The RN executes single-code Polar decoding algorithm for information retrieval. Therefore, in the following, we discuss the cases when the signals are overlapped, either partially or entirely. We then present our designs of the Polar decoding algorithm for information retrieval from the overlapped signals.

III. Polar Decoding Algorithms for Overlapped Transmissions

We use a vector form $\underline{g}_t$ to denote the bit(s) transmitted from the two SNs at time instant t, and $g_{t,j}$ is the jth component of $\underline{g}_t$. It is straightforward that

$$\underline{g}_t = \begin{cases} \left(x^{(0)}_t\right), & 0 \le t < \Delta\tau \\ \left(x^{(0)}_t, x^{(1)}_{t-\Delta\tau}\right), & \Delta\tau \le t < N \\ \left(x^{(1)}_{t-\Delta\tau}\right), & N \le t < N + \Delta\tau. \end{cases} \qquad (2)$$

The natural signaling in the system results in a mapping $\varphi_t : \mathbb{F}_2^{|\mathcal{L}_t|} \mapsto \mathcal{S}_t$ that maps a vector $\underline{g}_t \in \mathbb{F}_2^{|\mathcal{L}_t|}$ into $s_t = \varphi_t(\underline{g}_t) = \sum_{\ell\in\mathcal{L}_t} x^{(\ell)}_{t-\tau^{(\ell)}} \in \mathcal{S}_t$. We use $\underline{s} = (s_0, s_1, \ldots, s_{N+\Delta\tau-1})$ to denote the noiseless overlapped signals. Without loss of generality, we assume that the zeroth SN is allocated with higher power.

Upon receiving $\underline{y}$, the RN obtains $\Delta\tau$ and then recovers the information sequences by executing the following detection/decoding algorithms.

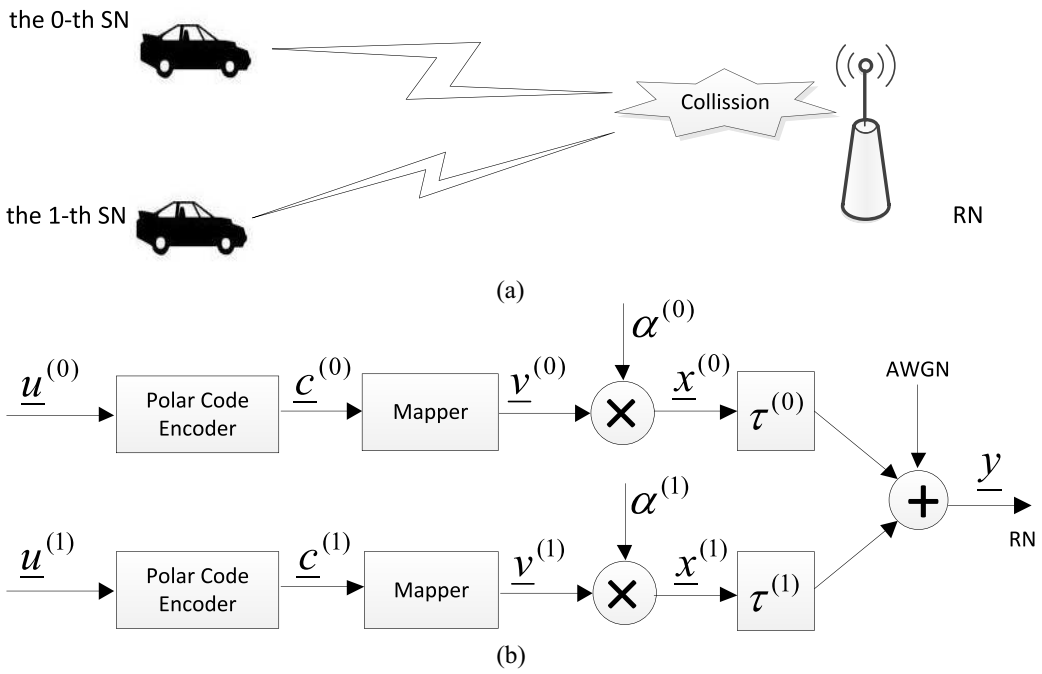

Fig. 3. System model. (a) Illustration of the communication system. (b) Schematic of the communication system.

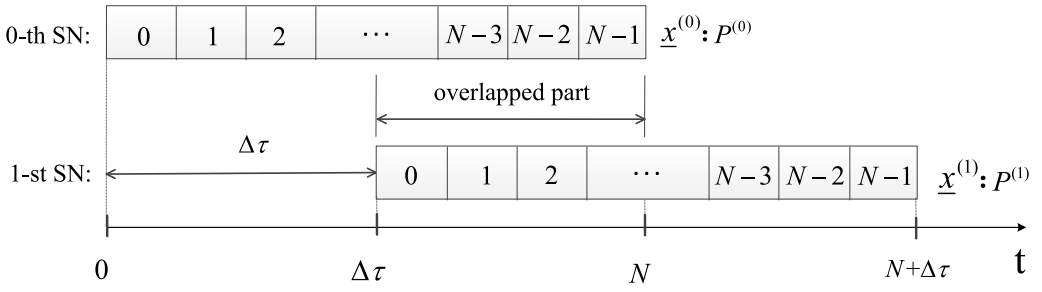

Fig. 4. Illustration of the overlapping model.

A. Iterative Soft Detection/Decoding Algorithm

In this section, we present an iterative soft detection/decoding algorithm (ISDA). A message associated with a random variable is defined by its probability mass function. For example, a message associated with a random variable Z over the finite filed $\mathbb{F}_q$ can be represented by $P_Z(z)$, $z \in \mathbb{F}_q$, a real vector of dimension q. For convenience, we use $P_{\underline{Z}}(\underline{z})$ to denote a sequence of messages, where the tth message corresponds to the tth random variable Z_t. We use the notation $P_{\underline{Z}}^{\mathrm{DEC}\to\Sigma}(\underline{z})$ to denote the messages from the decoder to the detector, and $P_{\underline{Z}}^{\Sigma\to\mathrm{DEC}}(\underline{z})$ to denote the messages from the detector to the decoder. To initialize the ISDA, we need the following original likelihoods:

$$f_t\left(y_t|\underline{g}_t\right) \propto \exp\left(-\frac{\|y_t-\varphi_t\left(\underline{g}_t\right)\|^2}{2\sigma^2}\right), \qquad \underline{g}_t \in \mathbb{F}_2^{|\mathcal{L}_t|} \tag{3}$$

for $0 \le t < N + \Delta\tau$.

It is known that belief propagation (BP) [27] and successive cancellation (SCAN) [28] are popular soft-in soft-out decoding algorithms of Polar codes. Compared with BP, the approach of SCAN has faster convergence rate and lower computation complexity. The ISDA for information retrieval from the overlapped signals is described in Algorithm 1. The ISDA can be executed with BP or SCAN as its soft-in soft-out decoder. We, respectively, call the algorithm BP-based ISDA or SCAN-based ISDA according to the type of soft-in soft-out local Polar decoder.

It is obvious that the main workload of this algorithm is the iteration processing. The time complexity is $O(|\mathcal{L}_t|N)$ at step 2.a) and $O(N\log_2 N)$ at step 2.b) [19]. Generally, the time complexity at step a) is much smaller than that at step b). Based on the maximum iteration number K, we known the total time complexity is $O(KN\log_2 N)$. At step 2.a), the space complexity is $O(N\log_2 N)$ and at other steps it is $O(N)$. Therefore, the final space complexity is $O(N\log_2 N)$.

B. Interference Elimination Decoding Algorithm

Due to power allocation, the zeroth SN's information received by the RN is more reliable than that of the first SN. Based on this observation, we present a successive cancellation list-based interference elimination decoding

Algorithm 1 ISDA

1. The messages $P^{\mathrm{DEC}\to\Sigma}_{\underline{C}^{(\ell)}}(\underline{c}^{(\ell)})$ are initialized with Bernoulli-1/2 distribution for $\ell = 0, 1$.
2. Select a maximum global iteration number K. For $k = 0, 1, \ldots, K-1$
   a) Detection: For $\ell = 0, 1$, compute the extrinsic messages $P^{\Sigma\to\mathrm{DEC}}_{\underline{C}^{(\ell)}}(\underline{c}^{(\ell)})$ with a soft-in-soft-out detector. The t-th component of $P^{\Sigma\to\mathrm{DEC}}_{\underline{C}^{(\ell)}}(\underline{c}^{(\ell)})$ is computed as
   $$P^{\Sigma\to\mathrm{DEC}}_{G_{t,i}}(m) \propto \sum_{\substack{\underline{g}_t\in\mathbb{F}_2^{|\mathcal{L}_t|}\\ g_{t,i}=m}} f_t\left(y_t|\underline{g}_t\right)\prod_{j\neq i} P^{\mathrm{DEC}\to\Sigma}_{G_{t,j}}\left(g_{t,j}\right), \tag{4}$$
   for $0 \le i \le |\mathcal{L}_t|$, $0 \le t < N + \Delta\tau$ and $m \in \mathbb{F}_2$.
   b) Decoding: For $\ell = 0, 1$, compute the extrinsic messages $P^{\mathrm{DEC}\to\Sigma}_{\underline{C}^{(\ell)}}(\underline{c}^{(\ell)})$ with a soft-in soft-out local decoder of Polar code.
3. Compute the full messages $P_{C_n^{(\ell)}}(c_n^{(\ell)}) \propto P^{\mathrm{DEC}\to\Sigma}_{C_n^{(\ell)}}(c_n^{(\ell)})P^{\Sigma\to\mathrm{DEC}}_{C_n^{(\ell)}}(c_n^{(\ell)})$ for $c_n^{(\ell)} \in \mathbb{F}_2$, $\ell = 0, 1$, and $0 \le n < N$. Then find
   $$\hat{c}_n^{(\ell)} = \arg\max_{c_n^{(\ell)}\in\mathbb{F}_2} P_{C_n^{(\ell)}}\left(c_n^{(\ell)}\right),$$
   for $\ell = 0, 1$, and $0 \le n < N$.

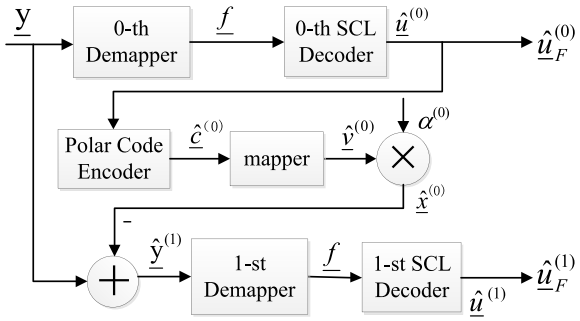

Fig. 5. Structure diagram of SCL-based IEDA.

Algorithm 2 SCL-Based IEDA

1. The channel bits probability of the 0-th SCL decoder is calculated by the 0-th demapper with
   $$f_t(y_t|m) \propto \sum_{\substack{\underline{g}_t\in\mathbb{F}_2^{|\mathcal{L}_t|}\\ g_{t,0}=m}} \exp\left(-\frac{\|y_t - \varphi_t\left(\underline{g}_t\right)\|^2}{2\sigma^2}\right), \tag{5}$$
   for $0 \le t < N$, and $m \in \{0, 1\}$.
2. The 0-th SCL decoder executes the SCL decoding algorithm with a list size L_0 and select only one decoding path with largest path metric to obtain the 0-th SN's estimated information sequence $\hat{\underline{u}}^{(0)}$.
3. Get the 0-th SN's estimated signal $\hat{\underline{x}}^{(0)}$ according to the $\hat{\underline{u}}^{(0)}$.
4. Subtract $\hat{\underline{x}}^{(0)}$ from the received signals to obtain the 1-st SN's estimated signal $\hat{\underline{y}}^{(1)}$ with noise.
   $$\hat{y}_t^{(1)} = \begin{cases} y_{t+\Delta\tau} - \hat{x}_t^{(0)}, & 0 \le t < N - \Delta\tau \\ y_{t+\Delta\tau}, & N - \Delta\tau \le t < N \end{cases}$$
5. For $0 \le t < N$, and $m \in \{0, 1\}$, the channel bits probability of SCL decoder is calculated with
   $$f_{l,t}\left(\hat{y}_{l,t}^{(1)}|m\right) \propto \exp\left(-\frac{\|\hat{y}_{l,t}^{(1)} - \alpha^{(1)}\phi_t(m)\|^2}{2\sigma^2}\right). \tag{6}$$
6. The 1-st SCL decoder executes the SCL decoding algorithm with a list size L_1 and select only one decoding path with largest path metric to obtain the 1-st SN's estimated information sequence $\hat{\underline{u}}^{(1)}$.
7. The final estimated information sequences $\{\hat{\underline{u}}_F^{(0)}, \hat{\underline{u}}_F^{(1)}\} = \{\hat{\underline{u}}^{(0)}, \hat{\underline{u}}^{(1)}\}$.

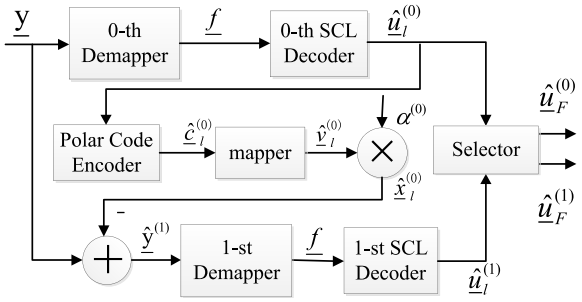

Fig. 6. Structure diagram of SCL-based IIEDA.

algorithm (SCL-based IEDA) for information retrieval of two SNs from the overlapped signals. The SCL-based IEDA first retrieves information from the zeroth SN, which is with higher power. Then the algorithm attempts to remove the interference from the zeroth SN to the first SN in the received overlapped signals. Subsequently, the first SN's information can be retrieved after the interference cancellation process. The traditional successive cancellation list (SCL) [26] algorithm is shown in [26]. The structure diagram of SCL-based IEDA is shown in Fig. 5 and the detailed descriptions of SCL-based IEDA are presented in Algorithm 2.

At all the steps except steps 2, 3, and 6 in SCL-based IEDA, the time complexity is $O(N)$. According to the analysis in [19] and [26], the time complexity are, respectively, $O(L_0 N \log_2 N)$ and $O(L_1 N \log_2 N)$ for both steps 2 and 6, the time complexity of step 3 is $O(N \log_2 N)$. Hence, the time complexity of this algorithm is $O((L_0 + L_1)N \log_2 N)$. Similarly, the space complexity of this algorithm depends on steps 2, 3, and 6. Therefore, the overall space complexity of SCL-based IEDA is $O((L_0 + \log_2 N + L_1)N)$.

The SCL decoding can be regarded as a breadth-first search algorithm on the code tree with a search width L [26]. However, there is only one estimated information sequence $\hat{u}_0$ with the largest path metric to be output. In order to provide more alternatives of estimated information sequences from the zeroth and the first SNs, we leave all the decoding paths $\hat{u}_l$, where $l = 0, 1, \ldots, L-1$. Next, we present an SCL-based IIEDA to improve system performance. The structure diagram of the SCL-based IIEDA is shown in Fig. 6. Detailed descriptions of the SCL-based IIEDA are given in Algorithm 3.

For each $l \in [0, L_0)$, the time complexity the of encoding process is $O(N \log_2 N)$ and the time complexity of SCL

Algorithm 3 SCL-Based IIEDA

1. The channel bits probability of the 0-th SCL decoder is calculated by the 0-th demapper with

$$f_t(y_t|m) \propto \sum_{\substack{\underline{g}_t \in \mathbb{F}_2^{|\mathcal{L}_t|} \\ g_{t,0}=m}} \exp\left(-\frac{\|y_t - \varphi_t(\underline{g}_t)\|^2}{2\sigma^2}\right), \tag{7}$$

for $0 \le t < N$, and $m \in \{0, 1\}$.

2. The 0-th SCL decoder execute the SCL decoding algorithm with a list size L_0 and leave all the L_0 decoding paths to obtain the 0-th SN's estimated information sequences $\hat{\underline{u}}_l^{(0)}$, $l = 0, 1, \ldots, L_0 - 1$.
3. For $l = 0, 1, \ldots, L_0 - 1$, do the following steps a $\rightarrow$ f.
   a. Get the 0-th SN's estimated signal $\hat{\underline{x}}_l^{(0)}$ according to the $\hat{\underline{u}}_l^{(0)}$.
   b. Subtract $\hat{\underline{x}}_l^{(0)}$ from the received signals to obtain the first SN's estimated signal $\hat{\underline{y}}_l^{(1)}$ with noise.

$$\hat{y}_{l,t}^{(1)} = \begin{cases} y_{t+\Delta\tau} - \hat{x}_{l,t}^{(0)}, & 0 \le t < N - \Delta\tau \\ y_{t+\Delta\tau}, & N - \Delta\tau \le t < N. \end{cases} \tag{8}$$

   c. For $0 \le t < N$, and $m \in \{0, 1\}$, the channel bits probability of SCL decoder is calculated with

$$f_{l,t}\left(\hat{y}_{l,t}^{(1)}|m\right) \propto \exp\left(-\frac{\|\hat{y}_{l,t}^{(1)} - \alpha^{(1)}\phi_t(m)\|^2}{2\sigma^2}\right). \tag{9}$$

   d. The 1-st SCL decoder executes the SCL decoding algorithm with a list size L_1 and select only one decoding path with largest path metric to obtain the 1-st SN's estimated information sequence $\hat{\underline{u}}_l^{(1)}$.
   e. Get the 1-st SN's estimated signal $\hat{\underline{x}}_l^{(1)}$ according to the $\hat{\underline{u}}_l^{(1)}$.
   f. For $0 \le t < N + \Delta\tau$, the estimated overlapped signal $\hat{\underline{s}}_l$ without noise is calculated with

$$\hat{s}_{l,t} = \sum_{\ell \in \mathcal{L}_t} \hat{x}_{l,t-\tau^{(\ell)}}^{(\ell)}. \tag{10}$$

4. For $l = 0, 1, \ldots, L_0 - 1$, the final estimated signals of the 0-th SN and the 1-st SN $\{\hat{\underline{x}}_F^{(0)}, \hat{\underline{x}}_F^{(1)}\}$ are selected by a selector with

$$\left\{\hat{\underline{x}}_F^{(0)}, \hat{\underline{x}}_F^{(1)}\right\} = \underset{\left\{\hat{\underline{x}}_l^{(0)}, \hat{\underline{x}}_l^{(1)}\right\}}{\arg\min} \|\underline{y} - \hat{\underline{s}}_l\|. \tag{11}$$

5. According to $\{\hat{\underline{x}}_F^{(0)}, \hat{\underline{x}}_F^{(1)}\}$, we get the corresponding final estimated information sequences $\{\hat{\underline{u}}_F^{(0)}, \hat{\underline{u}}_F^{(1)}\}$.

decoding processing for retrieval of first SN's information sequence is $O(L_1 N \log_2 N)$. Besides, the time complexity of other steps is $O(N)$. Therefore, the total time complexity is $O(L_0 L_1 N \log_2 N)$. Similar to the other two algorithms, the space complexity of SCL-based IIEDA is $O((L_0 + \log_2 N + L_1)N)$ because the main memory payload is the SCL-based decoding processing.

IV. Numerical Results

In the numerical examples, we used a rate 0.5 Polar code with different block lengths for simulation. From Examples 1 to 5, the transmission is over AWGN channel. In Example 6, practical channel characteristics of IoV is further considered, and Rayleigh fading channel with Doppler shift is adopted [29], [30]. BPSK modulation is adopted in all numerical examples. For comparison purposes, we assumed that the target frame error rate (FER) of the system is 10^{-3}, and the average transmission power $P = [(P^{(0)} + P^{(1)})/2]$ is normalized to 1. The signal-to-noise ratio (SNR) is defined as SNR $\triangleq 10\log_{10}(1/\sigma^2)$ dB, where σ^2 is the variance of AWGN.

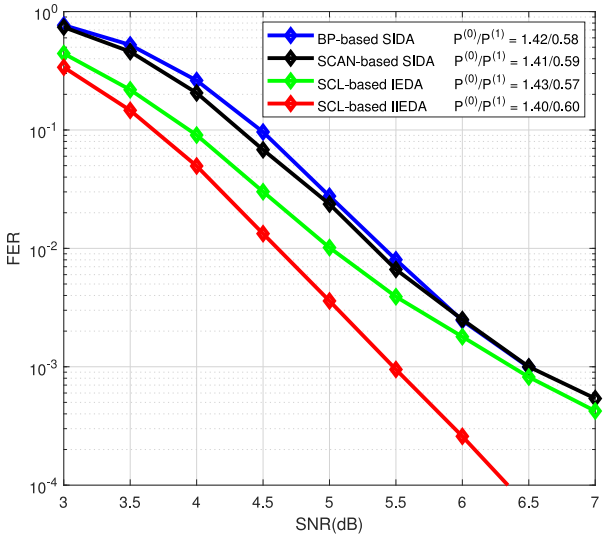

Fig. 7. FER performance comparison of different decoding algorithms in this paper with $\Delta\tau = 0$.

Through extensive simulations, we obtained the nearly optimal power allocation schemes for the proposed decoding algorithms. In the following examples, we are going to show performance of the proposed decoding algorithms from different perspectives.

Example 1: We first focus on the performance of the presented decoding algorithms in Section III in the entirely overlapping transmission with block length $N = 256$. Here, we examine the performance of the SCL-based IEDA and SCL-based IIEDA for comparison with BP-based ISDA and SCAN-based ISDA. Through extensive simulations, we find that the SCL-based IEDA has near optimal performance at FER $= 10^{(-3)}$ with power allocation $P^{(0)}/P^{(1)} = 1.43/0.57$. Meanwhile, the SCL-based IIEDA has the near optimal performance with $P^{(0)}/P^{(1)} = 1.40/0.60$. The near optimal power allocations of the BP-based and SCAN-based ISDAs are also obtained by simulations as shown in Fig. 7. The list sizes (L_0, L_1) of the SCL-based IEDA and SCL-based IIEDA are set to be 16. We set maximum global iteration number of the ISDA to $K = 8$, and the maximum local iteration numbers of BP and SCAN decoder are $I_{\mathrm{BP}} = 40$ and $I_{\mathrm{SCAN}} = 16$. As shown in Fig. 5, compared with BP-based ISDA and SCAN-based ISDA, it can be seen that SCL-based IIEDA has about 1.0 dB performance gains at FER $= 10^{-3}$. It can be also seen from Fig. 7 that SCL-based IIEDA has about 0.8 dB performance gain over that with SCL-based IEDA.

Example 2: Consider the situation when block length $N = 256$ and list sizes (L_0, L_1) are set to be 16 in the SCL-based

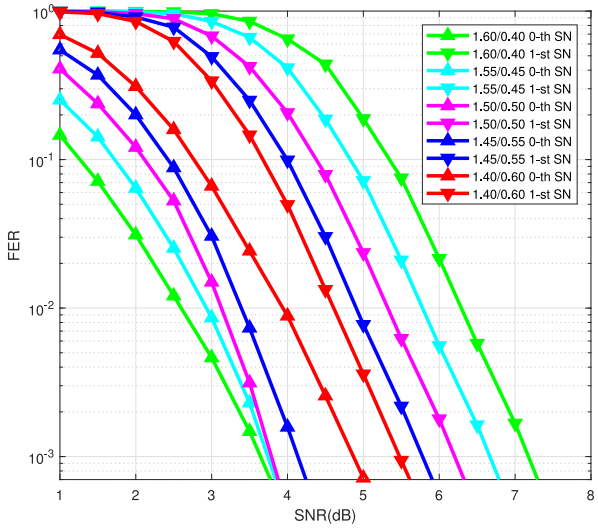

Fig. 8. FER performances of SCL-based IIEDA with different power allocations for the zeroth SN and the first SN.

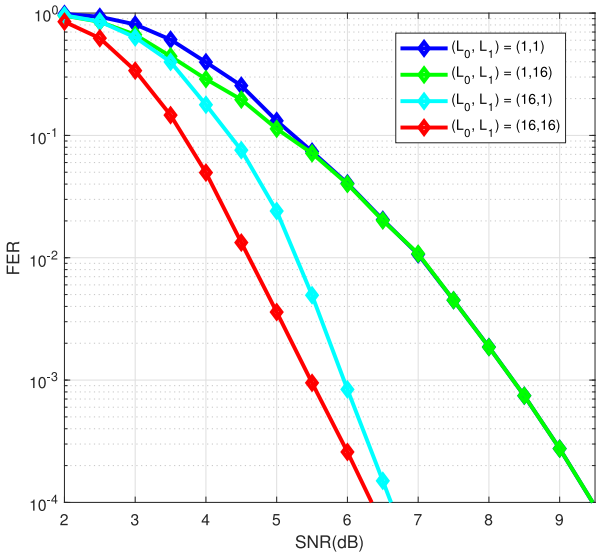

Fig. 9. FER performance comparison of SCL-based IIEDA with different list sizes (L_0, L_1), where $(L_0, L_1) = (1, 1)$, $(1, 16)$, $(16, 1)$, and $(16, 16)$.

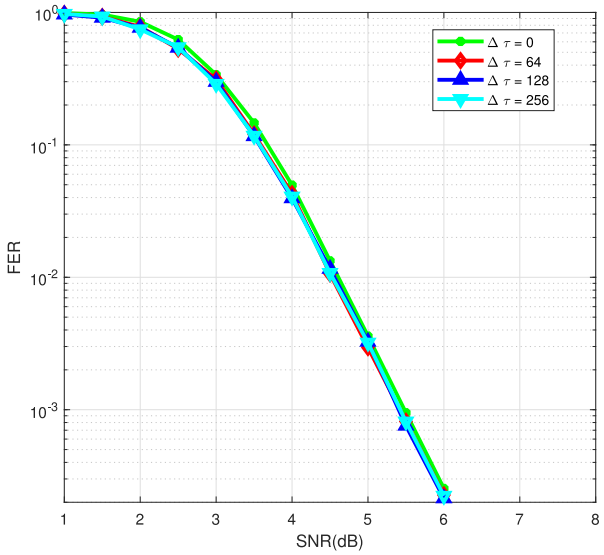

Fig. 10. FER performance comparison of SCL-based IIEDA with different $\Delta\tau$, where $\Delta\tau = 0, 64, 128$, and 256 and $N = 256$.

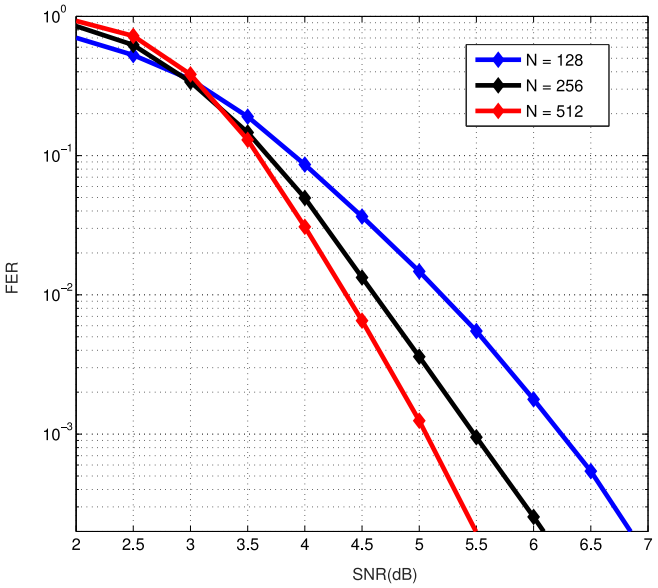

Fig. 11. FER performance comparison of SCL-based IIEDA with different block length N, where N = 128, 256, and 512.

IIEDA. We adjust the power allocation and then separately investigate the FER of the zeroth SN's information sequences and the first SN's to obtain Fig. 8. We notice from Fig. 8 that by choosing a proper energy allocation, we can narrow the FER performance gap between two SNs as far as possible.

Example 3: In this example, we investigate the FER performance comparison of SCL-based IIEDA with different list sizes (L_0, L_1). The (L_0, L_1) is varied from 1 to 16 to obtain Fig. 9. From Fig. 9, it can be observed that the FER performance is improved with the increase of L_0 or L_1. Compared the performance with list sizes $L_0 = L_1 = 1$, SCL-based IIEDA with list sizes $L_0 = L_1 = 16$ has about 2.8 dB performance gain at FER 10^{-3}.

Example 4: Here, we focus on the performance of SCL-based IIEDA with different relative delay $\Delta\tau$. From Fig. 10, it is observed that the decoding performance does not vary a lot with the change of $\Delta\tau$ and with the same $N = 256$. The correlation between decoding performance and $\Delta\tau$ is not obvious. It follows that SCL-based IEDA still performs well on information recovery no matter the signals are entirely overlapped or partially overlapped.

Example 5: In Fig. 11, FER performance comparison of SCL-based IIEDA with different block length, N = 128, 256, and 512, are shown. We see that as the block length N increases, the performance of SCL-based IIEDA improves.

Example 6: In Fig. 12, we simulated the proposed SCL-based IIEDA over Rayleigh fading channels with carrier frequency equal to 2.3 GHz and vehicle velocity of 120 km/h. In Fig. 12, we show performance of the SCL-based IIEDA algorithm in Rayleigh fading conditions with different block

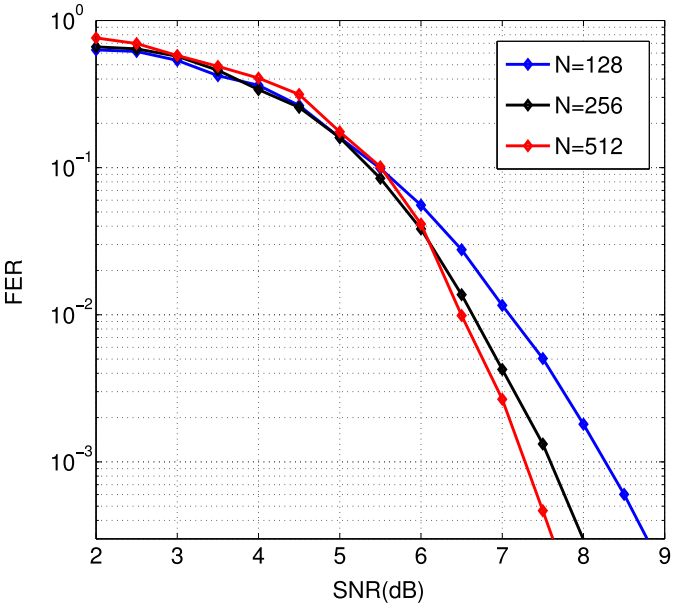

Fig. 12. FER performance comparison of SCL-based IIEDA with different block length N in Rayleigh channel, where N = 128, 256, and 512.

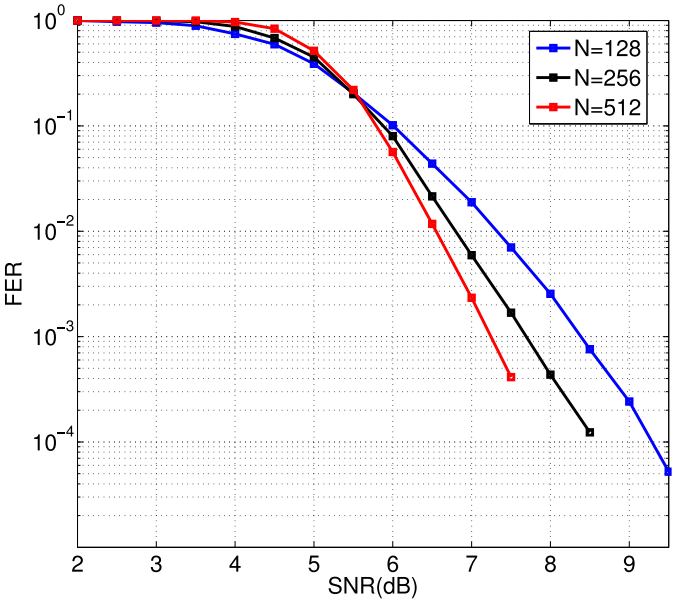

Fig. 13. FER performance comparison of SCL-based IIEDA with different block length N over wideband channel model for vehicle-to-vehicle communication system, where N = 128, 256, and 512.

length N. Retransmission has been activated when the channel fell into an extreme situation. The results show that the proposed overlapping scheme and Polar decoding algorithm worked well in practical IoV environments with Rayleigh fading and Doppler shift.

Example 7: To investigate the FER performance in more practical IoV environments, we further simulated the proposed SCL-based IIEDA over a wideband channel model for vehicle-to-vehicle communication system [30] with different block length N in Fig. 13. The speed of each Vehicle is about 120 km/h. The distance between the SN and the RN is about 200 m. The simulation results shows that the SCL-based IIEDA has similar performance as Example 6 with retransmission mechanism. When SNR is low, the worse channel causes the signal from first SN has not enough power for decoding. When SNR is larger, it is similar as Example 6. Because of the unbalance channel fading in the signals from different SNs, there are a little performance loss in Examples 6 and 7.

V. Conclusion

In this paper, we have presented an overlapping transmission scheme for IoV to facilitate high reliability low latency transmissions. Particularly, the nonorthogonal overlapping transmission significantly reduces overhead and latency due to the ACK mechanism for reliable receiving. In the proposed scheme, we have focused on a new decoding algorithm, namely the SCL-based IIEDA, for interference cancellation. In order to make a tradeoff between power saving and signal discrimination, we have analyzed the FER performance of power allocation rate. As the simulation results shown, the SCL-based IIEDA has given the near optimal performance with power allocation $P^{(0)}/P^{(1)} = 1.40/0.60$. Meanwhile, the SCL-based IIEDA has about 1 dB gain at FER $= 10^{-3}$ compared with ISDA and SCL-based IEDA. It is possible to retrieval information using power allocation while the two signals are highly overlapped. As shown in Fig. 10, the performance between nonoverlapping and entirely overlapping is close. In addition, the algorithm obtains better FER performance as the length of blocks increasing. To evaluate the performance in realistic channel, we simulated over a Rayleigh fading and Doppler shift channel as well as a wideband channel model for vehicle-to-vehicle communication system. The simulation showed, as the result of unbalance channel fading between different SNs and RN, the performance of decoding algorithm got some loss. There are two methods to avoid it. One is retransmission when the channel fading drops below a threshold. The other one is adaptive power allocation. They deserve much attention in the future study.

Acknowledgment

The authors would like to thank the anonymous reviewers, the Editor, Prof. N. Wang, and Dr. D. Zhang for their valuable comments and suggestions.

References

[1] F. Yang, S. Wang, J. Li, Z. Liu, and Q. Sun, "An overview of Internet of Vehicles," *China Commun.*, vol. 11, no. 10, pp. 1–15, Oct. 2014.

[2] M. Gerla, E.-K. Lee, G. Pau, and U. Lee, "Internet of Vehicles: From intelligent grid to autonomous cars and vehicular clouds," in *Proc. IEEE World Forum Internet Things*, Seoul, South Korea, Mar. 2016, pp. 241–246.

[3] X. Cheng, C. Chen, W. Zhang, and Y. Yang, "5G-enabled cooperative intelligent vehicular (5GenCIV) framework: When Benz meets Marconi," *IEEE Intell. Syst.*, vol. 32, no. 3, pp. 53–59, May/Jun. 2017.

[4] "Study on scenarios and requirements for next generation access technologies," 3GPP, Sophia Antipolis, France, Rep. TR 38.913, 2017.

[5] "IMT vision—Framework and overall objectives of the future development of IMT for 2020 and beyond," Int. Telecommun. Union, Geneva, Switzerland, ITU-Recommendation M.2083, Sep. 2015.

[6] D. Kombate and L. Wang, "The Internet of Vehicles based on 5G communications," in *Proc. IEEE Int. Conf. Internet Things*, Chengdu, China, Dec. 2016, pp. 445–448.

[7] B. M. Masini, A. Bazzi, and E. Natalizio, "Radio access for future 5G vehicular networks," in *Proc. IEEE Veh. Technol. Conf. Fall*, Toronto, ON, Canada, Sep. 2017, pp. 1–7.

[8] S.-L. Peng, G.-L. Lee, R. Klette, and C. H. Hsu, "Internet of Vehicles. Technologies and services for smart cities," in *Proc. 4th Int. Conf. (IOV)*, 2017, pp. 6, 55, 207, and 208.

[9] F. Zeng, R. Zhang, X. Cheng, and L. Yang, "Channel prediction based scheduling for data dissemination in VANETs," *IEEE Commun. Lett.*, vol. 21, no. 6, pp. 1409–1412, Jun. 2017.

[10] X. Cheng, L. Yang, and X. Shen, "D2D for intelligent transportation systems: A feasibility study," *IEEE Trans. Intell. Transp. Syst.*, vol. 16, no. 4, pp. 1784–1793, Aug. 2015.

[11] P. C. Newton and B. T. Sherin, "Dynamic backbone based broadcast technique for efficient bandwidth utilization in vehicular ad-hoc networks," *Indian J. Sci. Technol.*, vol. 10, no. 9, pp. 1–6, Mar. 2017.

[12] X. Xiao, L.-M. Yang, W.-P. Wang, and S. Zhang, "Wireless broadcasting retransmission approach based on network coding," *J. Commun.*, vol. 30, no. 9, pp. 782–786, Sep. 2009.

[13] G. Li, Q. Zhou, and J. Li, "A novel scheduling algorithm for supporting periodic queries in broadcast environments," *IEEE Trans. Mobile Comput.*, vol. 14, no. 12, pp. 2419–2432, Dec. 2015.

[14] P. A. Hoeher and T. Wo, "Superposition modulation: Myths and facts," *IEEE Commun. Mag.*, vol. 49, no. 12, pp. 110–116, Dec. 2011.

[15] J. Zhu, S. Zhao, and X. Ma, "A throughput enhanced transmission scheme for wireless sensor networks," in *Proc. Int. Conf. Wireless Commun. Signal Process.*, Yangzhou, China, Oct. 2016, pp. 1–5.

[16] S. Zhao, X. Ma, and B. Bai, "Decoding algorithms of LDPC coded superposition modulation," *IEEE Commun. Lett.*, vol. 18, no. 3, pp. 487–490, Mar. 2014.

[17] K. Ishii, "Cooperative transmit diversity utilizing superposition modulation," in *Proc. IEEE Radio Wireless Symp.*, Long Beach, CA, USA, Jan. 2007, pp. 337–340.

[18] E. G. Larsson and B. R. Vojcic, "Cooperative transmit diversity based on superposition modulation," *IEEE Commun. Lett.*, vol. 9 no. 9, pp. 778–780, Sep. 2005.

[19] E. Arikan, "Channel polarization: A method for constructing capacity-achieving codes for symmetric binary-input memoryless channels," *IEEE Trans. Inf. Theory*, vol. 55, no. 7, pp. 3051–3073, Jun. 2008.

[20] N. Hussami, S. B. Korada, and R. Urbanke, "Performance of polar codes for channel and source coding," in *Proc. IEEE Int. Symp. Inf. Theory*, 2009, pp. 1488–1492.

[21] Chairman Notes, *Chairmans Notes of Agenda Item 7.1.5 Channel Coding and Modulation*, document TSG RAN WG1 Meeting#87, 3GPP, Sophia Antipolis, France, Oct. 2016.

[22] E. Arikan, "Channel combining and splitting for cutoff rate improvement," *IEEE Trans. Inf. Theory*, vol. 52, no. 2, pp. 628–639, Jan. 2006.

[23] X. Cheng, C. X. Wang, B. Ai, and H. Aggoune, "Envelope level crossing rate and average fade duration of non-isotropic vehicle-to-vehicle Ricean fading channels," *IEEE Trans. Intell. Transp. Syst.*, vol. 15, no. 1, pp. 62–72, Feb. 2014.

[24] X. Cheng, C. X. Wang, D. Laurenson, S. Salous, and A. Vasilakos, "An adaptive geometry-based stochastic model for non-isotropic MIMO mobile-to-mobile channels," *IEEE Trans. Wireless Commun.*, vol. 8, no. 9, pp. 4824–4835, Sep. 2009.

[25] *Standard for Wireless Access in Vehicular Environments: Wireless LAN Medium Access Control (MAC) and Physical Layer (PHY)*, IEEE Standard 802.11p, Jul. 2010.

[26] I. Tal and A. Vardy, "List decoding of polar codes," *IEEE Trans. Inf. Theory*, vol. 61, no. 5, pp. 2213–2226, Aug. 2012.

[27] Y. Zhang, Q. Zhang, X. Pan, Z. Ye, and C. Gong, "A simplified belief propagation decoder for polar codes," in *Proc. IEEE Int. Wireless Symp.*, Xi'an, China, Mar. 2014, pp. 1–4.

[28] U. U. Fayyaz and J. R. Barry, "Low-complexity soft-output decoding of polar codes," *IEEE J. Sel. Areas Commun.*, vol. 32, no. 5, pp. 958–966, May 2014.

[29] X. Cheng *et al.*, "An improved parameter computation method for a MIMO V2V Rayleigh fading channel simulator under non-isotropic scattering environments," *IEEE Commun. Lett.*, vol. 17, no. 2, pp. 265–268, Jan. 2013.

[30] X. Cheng *et al.*, "Wideband channel modeling and ICI cancellation for vehicle-to-vehicle communication systems," *IEEE J. Sel. Areas Commun.*, vol. 31, no. 9, pp. 434–448, Jul. 2013.

Dalong Zhang received the Ph.D. degree in communication and information system from the Information Engineering University, Henan, China, in 2008.

He is currently an Associate Professor with the School of Information Engineering, Zhengzhou University, Zhengzhou, China. His current research interests include wireless communications networks, Internet of Vehicles, sensor networks, Internet of Things, and satellite positioning systems.

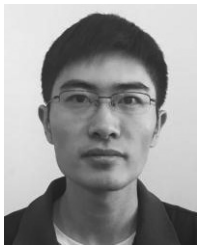

Liming Zheng received the B.E. degree in computer science from South China Normal University, Guangzhou, China, in 2016. He is currently pursuing the M.E. degree in computer science at Sun Yat-sen University, Guangzhou.

His current research interests include privacy and security in network communication, superposition transmission, and communication optimization in smart grids.

Qixiao Chen received the B.E. degree in communication engineering from Northeastern University, Shenyang, China, in 2016. He is currently pursuing the M.E. degree in electronic and communication engineering at Sun Yat-sen University, Guangzhou, China.

His current research interests include wireless communication networks, multiple access technology, superposition transmission, and Internet of Vehicles.

Baodian Wei received the Ph.D. degree in information and communication engineering from Xidian University, Shanxi, China, in 2004.

He is currently an Associate Professor with the School of Data and Computer Science, Sun Yat-sen University, Guangzhou, China. His current research interest includes cryptology and its applications.

Xiao Ma (M'08) received the Ph.D. degree in communication and information systems from Xidian University, Xi'an, China, in 2000.

He is a Professor with the School of Data and Computer Science, Sun Yat-sen University, Guangzhou, China. From 2000 to 2002, he was a Post-Doctoral Fellow with Harvard University, Cambridge, MA, USA. From 2002 to 2004, he was a Research Fellow with the City University of Hong Kong, Hong Kong. His current research interests include information theory, channel coding theory, and their applications to communication systems and digital recording systems.

Dr. Ma was a co-recipient, with A. Kavčíc and N. Varnica, of the 2005 IEEE Best Paper Award in Signal Processing and Coding for Data Storage and the Microsoft Professorship Award from Microsoft Research Asia in 2006.